CONTINUUM IONIZATION TRANSITION PROBABILITIES OF ATOMIC OXYGEN

JAMES A. R. SAMSON and V. E. PETROSKY

Behlen Laboratory of Physics, University of Nebraska, Lincoln, Neb. 68508

The technique of Photoelectron Spectroscopy has been used to obtain the relative continuum transition probabilities of atomic oxygen at 584 Å for transitions from the ^3P ground state into the ^4S, ^2D, and ^2P states of the ion. The ratio of the transition probabilities for the ^2D and ^2P states relative to the ^4S state of the ion are 1.57 ± 0.14 and 0.82 ± 0.07, respectively. In addition, transitions from the excited $O_2(a\ ^1\Delta_g)$ state into the O_2^+ ($^2\Phi_u$ and $^2\Delta_g$) states were observed. The adiabatic ionization potential of O_2^+ ($^2\Delta_g$) was measured as 18.803 ± 0.006 eV.

INTRODUCTION

Many theoretical investigations of the photoionization of atomic oxygen have been carried out.[1-8] These include cross section calculations, transition probabilities for specific ionic states, and calculations of the angular distribution of the ejected photoelectrons. The experimental verification of these calculations is difficult because of the experimental problems in dealing with a transient species such as atomic oxygen. In addition to supporting a particular theoretical model the experimental results on the photoionization of atomic oxygen are extremely important in upper atmospheric studies since a prime constituent of the Earth's atmosphere at about 200 km is atomic oxygen.

Previous experimental studies on photon interaction with atomic oxygen have been confined to absorption studies. Huffman et al.[9] obtained an absorption spectrum between 600 and 1000 Å while Cairns and Samson[10] and Comes and Elzer[11] measured absolute cross sections at discrete emission lines in the same wavelength interval. More recently Jonathan et al.[12,13] have observed the photoelectron spectrum of atomic oxygen at 584 Å and Dehmer et al.[14] have studied the ions produced by photoionization in a mass spectrometer.

The present investigation involves the technique of photoelectron spectroscopy. This is an extremely powerful method for measuring the relative transition probabilities for populating the various ionic states available for the given photon energy. However, to obtain meaningful results the collection efficiency of the electron energy analyzer must be calibrated as a function of the electron energy and the analyzer must not discriminate against electrons with differing angular distributions. To

date this has not been done. The present work reports absolute transition probabilities for the photoionization transition $2p^4(^3P) \rightarrow 2p^3(^2D, ^2P) + e$ relative to transitions to the $2p^3(^4S)$ ground state of the atomic oxygen ion.

EXPERIMENTAL

Atomic oxygen was produced in a microwave discharge (2450 MH) operating at a power of 40 W and at a pressure of approximately 20 m Torr. Although number densities of the atoms were not measured similar techniques have produced about 5% dissociation.[10] In addition to atomic oxygen other species were produced. The parent molecule can be excited into the lowest excited state, the $O_2(a\ ^1\Delta_g)$ state, which lies about 1 eV above the ground $X\ ^3\Sigma_g$ state. Molecules in the excited $a\ ^1\Delta_g$ state account for about 5 to 10 percent of the products. Other species may be formed such as ozone and O_2 in various vibrational states. However, these were not observed in the present experiment where the discharged gas had to travel about 50 cm through 11 mm id pyrex tubing. Quartz tubing was used in the microwave cavity. The tubing was treated with dilute phosphoric acid to minimize the recombination of atomic oxygen. Thus, three species were formed, namely, $O\ (^3P)$, $O_2\ (X\ ^3\Sigma)$, and $O_2\ (a\ ^1\Delta_g)$. Figure 1 shows the microwave discharge and the atomic oxygen flow in relation to the photoelectron spectrometer.

The electron energy analyzer was a cylindrical mirror design based on the analysis given by Karras et al.[15] Slit to slit focusing was adopted with an entrance trajectory of 54.7° with respect to the axis of the cylinders. This particular angle was chosen because the fraction of the electrons travelling in this direction is directly proportional to the total number of photoelectrons produced regardless of their angular distribution.[16] A

retarding/accelerating lens (L) was incorporated so that the electrons would have a fixed pass energy and hence a constant energy resolution. With 2 volts between the inner and outer cylinders the full width at half maximum for argon was 30 meV. The supporting discs for mounting the inner and outer cylinders were made from Plexiglass. The surfaces facing the analyzing region were coated with a thin layer of vacuum evaporated tellurium. Electrical contact was made with silver conducting paint. When the analyzing voltage was applied a logarithmic field was set up matching that between the cylinders. With this continuous fringing field corrector the supports could be located very close to the slits (about 0.5 cm). Helmholtz coils were used to reduce the Earth's field in the analyzer to a few milligauss.

To measure the probability for transitions into the various ionic states it is essential that the analyzer be calibrated for its response to electrons of various energies. The effect of stray magnetic fields, contact potentials, and detector response may vary with the kinetic energy of the electrons. In addition the transmission of the retarding/accelerating lens will be a function of electron energy. All of these factors were accounted for by measuring the collecting efficiency of the entire analyzer as a function of electron energy. Because the analyzer did not discriminate against electron groups with different angular distributions the calibration was achieved by simply measuring the branching ratios of the various electronic and vibrational states of several gases (O_2, N_2, and CO_2). The observed branching ratios were compared (and corrected) with the true branching ratios.[17] The correction factor, as a function of electron energy, produced the desired collection efficiency curve (see Fig. 2).

The 584 Å radiation was produced by an undispersed glow discharge in helium. The helium was purified by passing it through a zeolite trap cooled

by liquid nitrogen. The light source was first tested on a ½ m Seya vacuum uv monochromator to determine the intensity of the other members of the HeI resonance series and also to check for possible impurity lines. The most intense line, in addition to the 584 Å line, was the second member of the He series, the 537 Å line. However, the 537 Å line was about a factor of 50 less intense than 584 Å. If a small air leak is present in the source some very weak OI resonance lines are produced (about 200 times weaker than 584 Å). However, these resonance lines are highly reabsorbed by the atomic oxygen in the analyzer. The states subsequently autoionize and produce strong spurious signals. A discussion of this phenomena is presented in detail elsewhere.[18]

RESULTS

Figure 3 shows the photoelectron spectrum of O_2 with and without the discharge. The atomic states are clearly seen. In addition, transitions from the excited O_2 $^1\Delta_g$ state are observed. The transition O_2 ($a\ ^1\Delta_g$) → O_2^+ ($X\ ^2\Pi$) is clearly identified. This gives an ionization potential of the $a\ ^1\Delta_g$ state 1.00 eV below that of the O_2 ($X\ ^3\Sigma_g$) ground state. This value is in agreement with previously published values.[10,19-21] Transitions from the $a\ ^1\Delta_g$ state into higher lying levels of the ion are also observed. These have been identified by Jonathan et al. as transitions into the $^2\Phi$ and $^2\Delta$ ionic states.[13,22] These states are shown in more detail in Fig. 4. The adiabatic ionization potential for the transition O_2 ($a\ ^1\Delta_g$) → O_2^+ ($^2\Delta_g$) obtained from the present work is 18.803 ± 0.006 eV. The vibrational spacing of the $^2\Delta_g$ state is 116 ± 5 mV. This is in excellent agreement with the results of Jonathan et al.[13] The $^2\Phi_u$ state is not clearly resolved but an estimate of its vibrational spacing is ~ 110 mV and one vibrational peak has

an energy of 18.250 eV.

The technique used to obtain the intensity of the ^2D transition was to take peak heights of the $v = 6$, 7, and 8 vibrational levels of the a $^4\Pi$ state with the discharge on and off. This establishes the relative intensities of the vibrational levels and the excess signal in the $v = 7$ level with the discharge on is the contribution to the O^+ (^2D) state. The peak heights of the ^4S, ^2D, and ^2P states, as shown in Fig. 3, must be corrected for the collection efficiency of the analyzer (see Fig. 2). The results for the transition probabilities of the ^2D and ^2P states relative to the ^4S ground state of the ion are given in Table I along with the results of several theoretical calculations. Most of the calculations lie within ± 10% of the experimental data. However, the results of Henry, who used close-coupled wave functions to describe the final continuum orbitals, show the closest agreement with experiment.

ACKNOWLEDGMENTS

This work was supported in part by the National Science Foundation and the National Aeronautics and Space Administration under grants No. GA-36718 and NGR 28-004-021.

REFERENCES

1. A. Dalgarno and D. Parkinson, J. Atmosph. Terr. Phys. 18, 335 (1960).
2. A. Dalgarno, R. J. W. Henry, and A. L. Stewart, Planet. Space Sci. 12, 235 (1964).
3. R. J. W. Henry, Planet. Space Sci. 15, 1747 (1967).
4. G. M. Thomas and T. M. Helliwell, J. Quant. Spectrosc. Radiat. Transfer 10, 423 (1970).
5. H. Kahler, J. Quant. Spectrosc. Radiat. Transfer 11, 1521 (1971).
6. P. S. Ganas, Phys. Rev. 7, 928 (1973).
7. D. J. Kennedy, S. T. Manson, and A. Starace, Planet. Space Sci. (to be published).
8. S. T. Manson and A. Starace, Phys. Rev. (to be published).
9. R. E. Huffman, J. C. Larrabee, and Y. Tanaka, J. Chem. Phys. 46, 2213 (1967). See also, Phys. Rev. Letters 16, 1033 (1966) and J. Chem. Phys. 47, 4462 (1967).
10. R. B. Cairns and J. A. R. Samson, Phys. Rev. 139, A1403 (1965).
11. F. J. Comes, F. Speier, and A. Elzer, Z. Naturforsch. A23, 125 (1968).
12. N. Jonathan, A. Morris, D. J. Smith, and K. J. Ross, Chem. Phys. Letters 7, 497 (1970).
13. N. Jonathan, A. Morris, M. Okuda, K. J. Ross, and D. J. Smith (to be published).
14. P. M. Dehmer, J. Berkowitz, and W. A. Chupka, J. Chem. Phys. (to be published).
15. M. Karras, M. Pessa, and S. Aksela, Ann. Acad. Sci. Fenn. AVI, 289 (1968).
16. J. A. R. Samson and J. L. Gardner, J. Opt. Soc. Am. 62, 856 (1972).
17. J. A. R. Samson and J. L. Gardner, unpublished data.

18. J. A. R. Samson and V. E. Petrosky, to be published.

19. S. N. Foner and R. L. Hudson, J. Chem. Phys. 25, 601 (1956).

20. R. J. McNeal and G. R. Cook, J. Chem. Phys. 45, 3469 (1966).

21. N. Jonathan, D. J. Smith, and K. Ross, J. Chem. Phys. 53, 3758 (1970).

22. N. Jonathan, A. Morris, K. J. Ross, D. J. Smith, J. Chem. Phys. 54, 4954 (1971).

TABLE I. Relative transition probabilities of the ^2D and ^2P ionic states of atomic oxygen relative to the ^4S ground state of the ion.

	$^2D/^4S$	$^2P/^4S$	references
This work	1.57 ± 0.14	0.82 ± 0.07	
Manson and Starace	1.49	0.96	(8)
Henry	1.53 (DV)	0.91 (DV)	(3)
	1.57 (DL)	0.85 (DL)	
Dalgarno et al.	1.20 (DV)	0.74 (DV)	(2)
	1.41 (DL)	0.98 (DL)	
Kahler	1.45	0.90	(5)
	1.65	1.05	
*Ganas	0.7	0.24	(6)
*Thomas and Helliwell	1.5	0.8	(4)

*Estimated values from published total cross sections.

DV and DL denote, respectively, dipole velocity and dipole length approximations.

Figure Captions

1. Cylindrical mirror electron energy analyzer. L is the retarding/accelerating lens and C is the channeltron detector. The microwave discharge, for the production of atomic oxygen, is shown in relation to the analyzer.

2. Analyzer collection efficiency as a function of electron energy.

3. Photoelectron spectrum of O_2 (upper curve), and photoelectron spectrum of the discharged products $O(^3P)$, $O_2(^3\Sigma)$, and $O_2(^1\Delta_g)$. The dashed vertical line denotes the position 21.218 eV, which is the energy of the 584 Å line (lower curve).

4. Photoelectron spectrum of discharged O_2 between 18 and 19 eV. The $O^+ {}^2P$ level is clearly resolved from the $v = 3$ vibrational state of the $O_2^+(b\ {}^4\Sigma)$ state. The transitions $O_2(a\ {}^1\Delta_g) \rightarrow O_2^+({}^2\Phi_u$ and $ {}^2\Delta_g)$ are indicated.

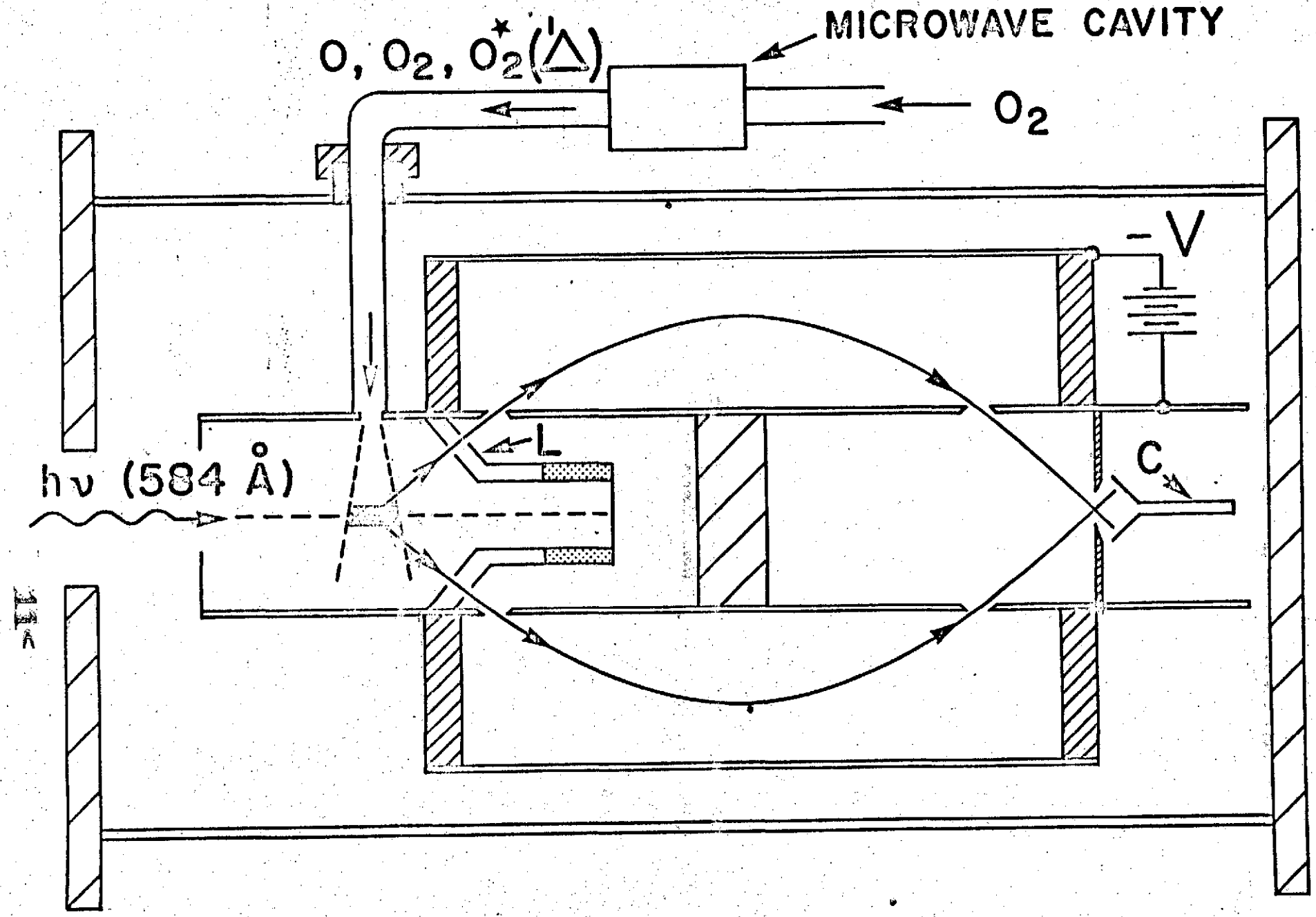
MICROWAVE CAVITY
O, O2, O2*(1Δ)
O2
-V
L
hν (584 Å)
C

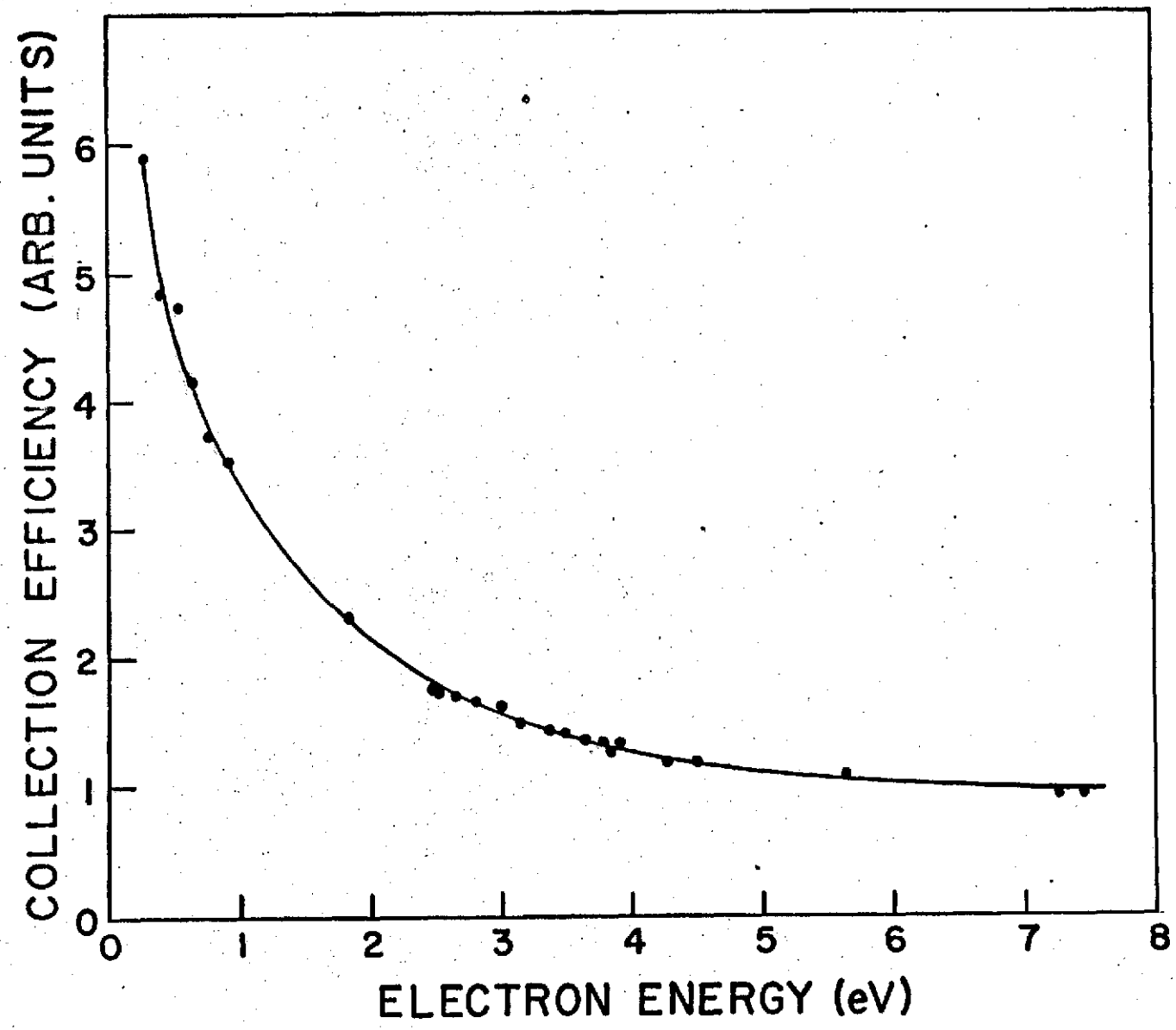
COLLECTION EFFICIENCY (ARB. UNITS)
0
1
2
3
4
5
6
0
1
2
3
4
5
6
7
8
ELECTRON ENERGY (eV)

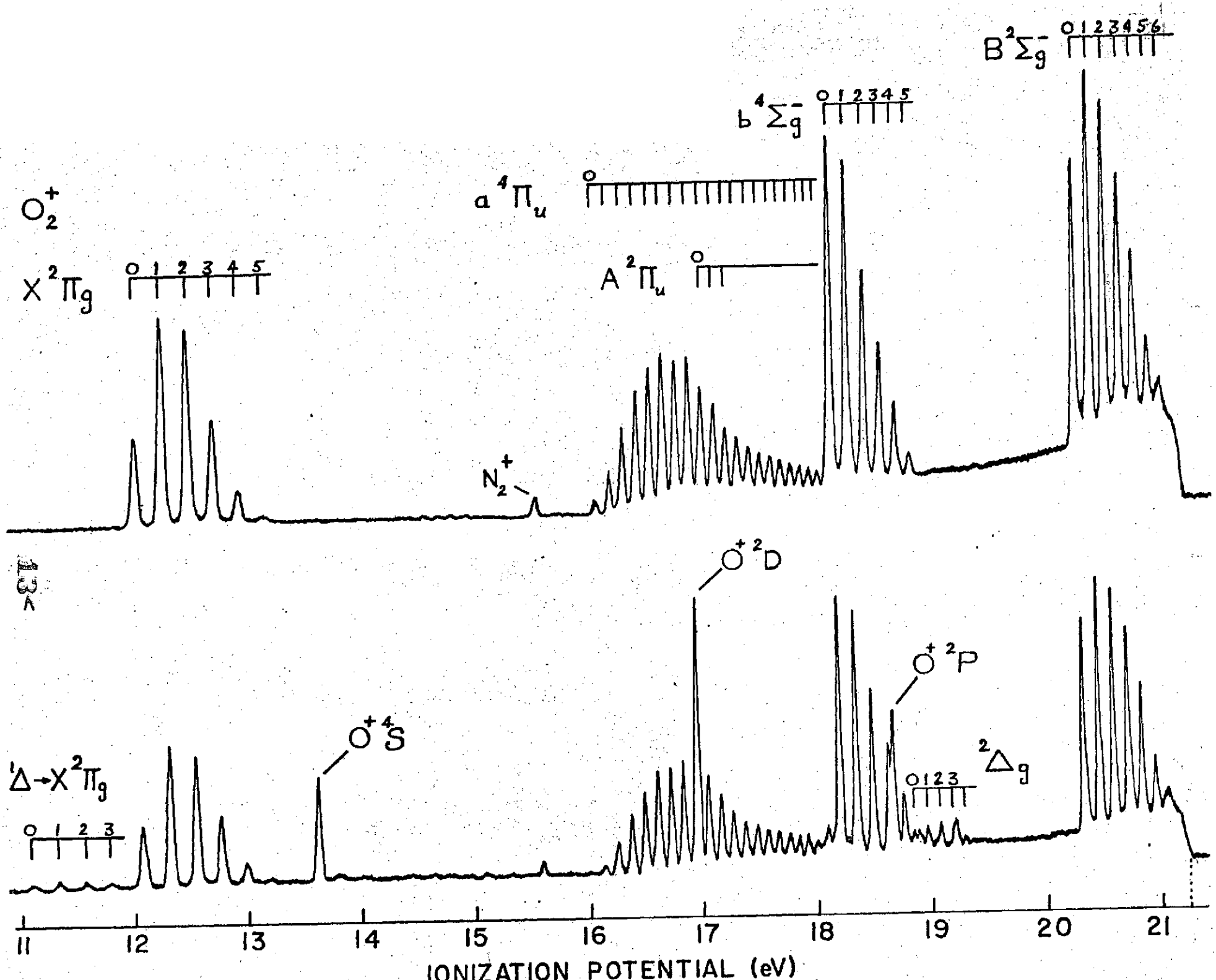
O_2^+
$X^2\Pi_g$
0 1 2 3 4 5
$a^4\Pi_u$
$A^2\Pi_u$
$b^4\Sigma_g^-$
0 1 2 3 4 5
$B^2\Sigma_g^-$
0 1 2 3 4 5 6
N_2^+
$O^+ {}^4S$
$O^+ {}^2D$
$O^+ {}^2P$
$^2\Delta_g$
0 1 2 3
$^1\Delta \rightarrow X^2\Pi_g$
0 1 2 3
11
12
13
14
15
16
17
18
19
20
21
IONIZATION POTENTIAL (eV)

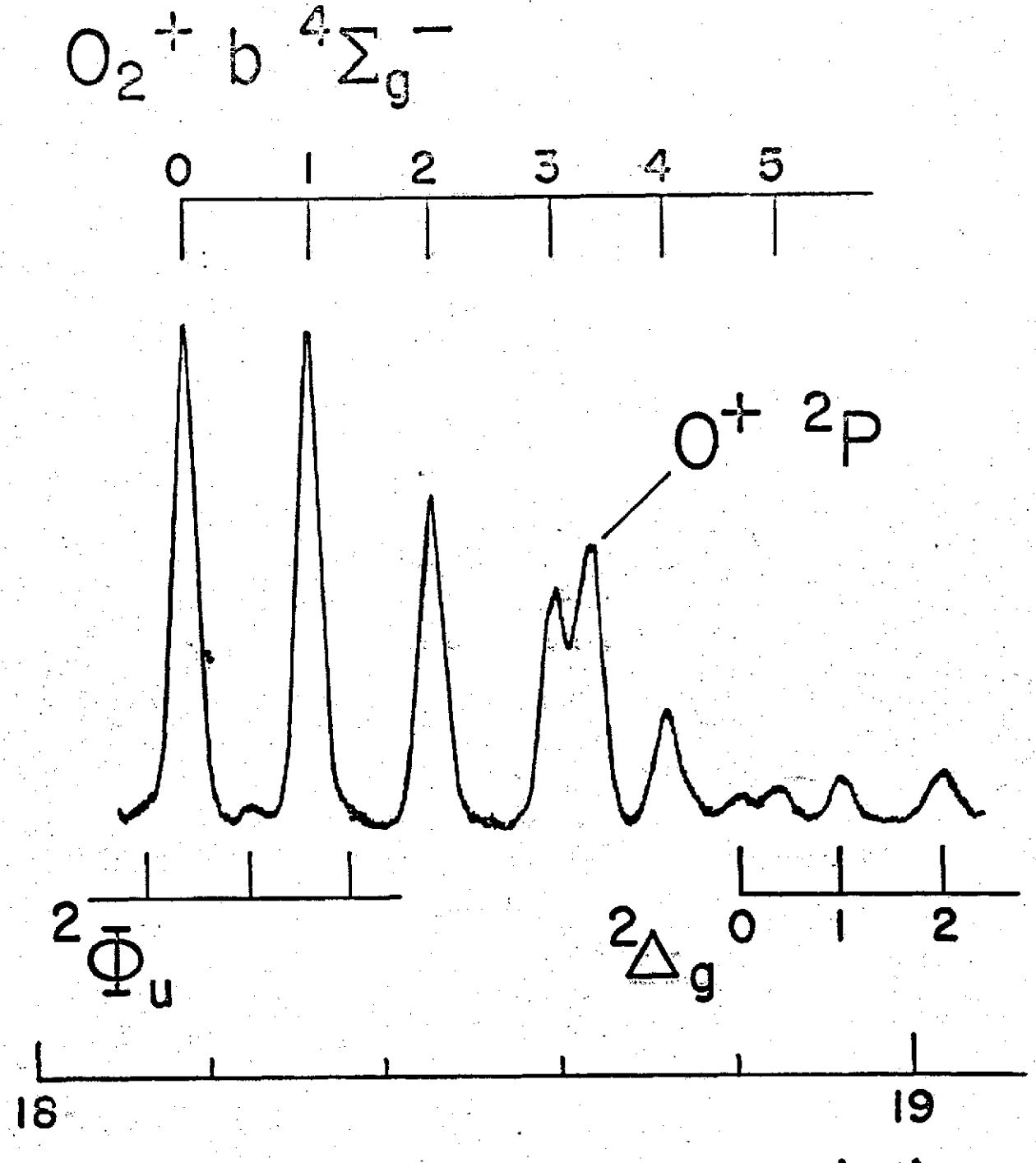
O_2^+ b $^4\Sigma_g^-$
0 1 2 3 4 5
O^+ ^2P
$^2\Phi_u$
$^2\Delta_g$
0 1 2
18
19
IONIZATION POTENTIAL (eV)